N87-23322

CURRENT DRIVEN WEAK DOUBLE LAYERS

Gérard Chanteur
CRPE/CNET, 92131 Issy-les-Moulineaux, France

ABSTRACT

Double layers in plasmas can be created by different means. For example, a potential difference forms between two plasmas with different temperatures (Hultqvist, 1971; Ishiguro et al., 1985), in a plasma jet flowing along a converging magnetic field (Serizawa and Sato, 1984), in a quiescent plasma submitted to an external difference of potential, or in a turbulent plasma carrying an electric current. The first three cases can be current-free, but not necessarily, although the numerical simulations have been made under such conditions for the first two points (Ishiguro et al., 1985; Serizawa and Sato, 1984). Apart from the third case, which is mainly of interest for laboratory experiments, these double layers are good candidates for accelerating the auroral electrons to the few kiloelectron volts observed.

I. INTRODUCTION

This paper is devoted to the fourth case, i.e., to weak double layers driven by an electric current. Two papers have triggered the studies in this field: DeGroot et al. (1977) showed the formation of localized potential jumps in an homogeneous plasma with a suprathermal electron drift; later, Sato and Okuda (1980) gave evidence for the formation of small double layers under ion-acoustic instability conditions, i.e., a large electron-to-ion temperature ratio and a subthermal electron drift. Our present understanding of weak double layers built by electric currents has mainly grown from the analysis of numerical simulations with either superthermal (DeGroot et al., 1977; Singh et al., 1985; Singh and Schunk, 1984) or subthermal (Sato and Okuda, 1980, 1981; Kindel et al., 1981; Hudson and Potter, 1981; Okuda and Ashour-Abdalla, 1982; Hasegawa and Sato, 1982; Nishihara et al., 1982; Chanteur et al., 1983; Chanteur, 1984, 1986; Barnes et al., 1985) electron drifts, but always in linearly unstable conditions. The formation mechanism seems to be different in these two cases; furthermore, it is likely to be sensitive to the boundary conditions in the superthermal case. The basic mechanism which produces weak ion-acoustic double layers is a current interruption caused by a negative potential spike. This fact was primarily recognized in one-dimensional periodic simulations (Sato and Okuda, 1981; Kindel et al., 1981; Hasegawa and Sato, 1982; Nishihara et al., 1982; Chanteur et al., 1983) and has been recently confirmed in the two-dimensional case with a strong magnetic field and under various boundary conditions (Barnes et al., 1985). The theoretical explanation given to the appearance and the growth of a double layer (Hasegawa and Sato, 1982; Nishihara et al., 1982; Chanteur et al., 1983; Chanteur, 1984) turns out to be more or less independent of the linear instability. The goal of this paper is to specify this point, and it will be shown that small and localized differences of potential can be built by a partial current interruption under linearly stable conditions. It has been demonstrated (Dupree, 1983; Berman et al., 1985; Pécseli, 1984) that phase space holes can be unstable for electron drifts less than the critical value which destabilizes the ion-acoustic modes. Although different from our work in many respects, it invokes the same physical basis, i.e., the reflection of the current carrying electrons by coherent structures. Section II gives an account of the formation of weak ion-acoustic double layers under linearly unstable conditions. Section III is a first presentation of recent simulations demonstrating that small double layers can be produced by a localized current interruption in a marginally stable plasma. A more thorough presentation of these numerical experiments is in preparation (Verga et al., 1986).

II. UNSTABLE CASE

Most of the numerical studies concerning ion-acoustic double layers have been made with electrostatic particle codes that allow for the existence of thermal fluctuations. Indeed, the relatively small number of particles per Debye length (usually a few 10^1 or 10^2) gives rise to an artifically high level of thermal fluctuations. Besides, the probability of "big" fluctuations of the electric potential increases with the length of the system and should not be dismissed. Since ion-acoustic waves are weakly dispersive, we can argue that a big and negative potential spike present in the "initial" condition has a coherence time long enough to interact resonantly with the electrons. The word "initial" deserves a short explanation: a particle run is usually started with particles regularly distributed in space and attributing each particle a velocity given by a random number generator. The electric field usually taken equal to zero everywhere at $t = 0$ is built self-consistently by the thermal motion of the particles in a few tens of time steps. It appears that the "initial" condition on the field is determined by the microscopic details of the loading of the particles. The longer the system, the greater the probability to find a negative potential spike sufficiently above the thermal level to produce a persistent interruption of the current by reflecting the electrons. In a short and periodic system without any externally applied electric field, this current interruption goes on for the transit time of the electron flow through the system and a stable BGK state results with a large fraction of trapped electrons. If the system is long enough for the establishment of this BGK state to be delayed and if the negative spike is not too close downstream of another big spike, the evolution will be qualitatively different, giving rise to a weak and transient double layer, as will be seen below. Increasing the length of the system, we increasee the probability of the large fluctuations and delay the appearance of the BGK state; the combination of these two facts is likely to explain both the reason why double layers have never been observed in short periodic systems and the reason for the mean distance between double layers in very long systems. Instead, open boundary conditions not only provide a continuous input of energy into the system but new potential fluctuations are usually created near the input boundary (i.e., where the incoming flux of electrons is greater) and propagate through the system, giving rise to the observed temporal recurrence of double layers even in short open systems (Barnes et al., 1985). Consequently, the spatial and temporal recurrences of double layers in open systems are mainly governed by the chosen injection process of the particles at the boundaries. On the other hand, it has been shown (Barnes et al., 1985) that the formation mechanism of a weak double layer reported in detail in Nishihara et al. (1982), Chanteur et al. (1983), Chanteur (1984, 1986), and Barnes et al. (1985) is independent of the boundary conditions. Let us now recall the main features of this process.

In a system driven unstable by an electric current, the perturbations propagating against the electron flow are strongly damped, and the perturbations close to the most unstable wave number are rapidly selected among the other ones. On the basis of the linear instability theory for an homogeneous plasma, we expect the turbulence to develop homogeneously. Instead, it is observed that the evolution of long systems is dominated by one or few coherent structures, as was shown initially by Sato and Okuda (1980). For example, Figure 1 shows a negative potential spike (the figure in fact represents the potential energy of an electron), with $e\phi/T_e \sim 1$ which has emerged from the thermal noise in a one-dimensional electrostatic and periodic particle simulation with the following parameters: length $L = 512\ \lambda_D$, ion-to-electron mass ratio $m_i/m_e = 100$, electron-to-ion temperture ratio $T_e/T_i = 20$, and electron drift to thermal speed ratio $V_d/V_{th} = 0.8$. As previously discussed, this pulse originates in a thermal fluctuation present in the "initial" condition. This negative spike of potential is initially amplified by the linear instability taken over by the nonlinear instability discussed in Nishihara et al. (1982) and Chanteur (1983). The electrons having a kinetic energy less than the height of the potential barrier are reflected on both sides of the pulse; yet, due to the current, more electrons impinge on the left side of the barrier than on the right side and, consequently, more electrons are reflected upstream of the barrier than downstream. This simple fact has important implications. First, the resulting charge separation in the vicinity of the barrier develops a difference of potential between the two sides of the pulse, as can be seen around $x = 120\ \lambda_D$ in Figue 1, the low electric potential being on the upstream side of the barrier (upstream with respect to the electron drift). Second, quasi-neutrality of the plasma being preserved outside of the pulse, the electron density in excess on the upstream side is compensated for by an increased ion

density. Thus, the deep density trough associated with the potential pulse separates the upstream region of inflated plasma density from the depleted downstream region. Third, taking into account the velocity of the barrier, the mechanism of the instability can be easily understood. Let $\vec{V}_o$ be the velocity of the barrier and $\vec{V}$ the velocity of an incoming electron in the frame of reference moving with the barrier; assuming that the potential does not change during the interaction with this electron (a reasonable assumption considering the time scales in the numerical experiments), the collision is elastic and the particle leaves with a velocity $-\vec{V}$. The kinetic energy of the particle in the laboratory frame has changed from $1/2\ m_e(\vec{V}_o + \vec{V})^2$ to $1/2\ m_e(\vec{V}_o - \vec{V})^2$; i.e., an energy $2m_e\ \vec{V}_o.\vec{V}$ has been transferred to the barrier. The potential barrier moving primarily in the direction of the electron flow receives more energy from the electrons impinging on the upstream side than it gives the downstream side, and the field energy locally grows! Detailed energy and momentum balances have been made theoretically (Nishihara et al., 1982; Chanteur et al., 1983; Pecseli, 1984) and checked in the simulations (Chanteur et al., 1983).

Due to the relatively small number of particles per Debye length, local diagnostics in phase space (for example the distribution function of electrons at a given location) are poorly done in particle simulations. Instead, Vlasov simulations are free of this limitation, but in return suffer, at least for this study, from the absence of thermal noise. Starting with an initial condition strictly independent of x, a good Vlasov code can be run a long time before truncation and round-off errors seed a potential instability. An initial perturbation has to be put, whether random or not, in the system; an account of weak double layer formation under such circumstances has been given in Chanteur (1984). For the present discussion, we just recall the simulation presented in Chanteur et al. (1983). This Vlasov run was initialized with the same physical parameters as the aforementioned particle run, the initial perturbation being a localized 10 percent density depression on both species. Although qualified "perhaps unphysical" in Borovsky (1984), this initial condition reproduces what is built from the exaggerated thermal noise present in particle simulations. In fact, the potential energy of an electron shown versus x and t in Figure 2 is strinkingly similar to the result of the particle simulation (see Fig. 1). This temporal evolution of the system is not an artifact of the periodic boundary conditions; doubling the length of the system while keeping the same physical parameters does not change anything. On the other hand, this behavior is also observed in bounded systems and for different physical parameters (Barnes et al., 1985). Thus, it is not due either to some numerical coincidence for a magic set of parameters; in turn, the boomerange motion of the localized wave seems to be an artifact of one-dimensionality (Barnes et al., 1985). Figure 3 displays the electron phase space in the vicinity of the double layer at three different times during its propagation in the direction of the electron flow. The reflections of the electrons are clearly visible on both sides of the structure, and the electron holes are seen to be formed in the depleted downstream region [see also Chanteur (1984) and Barnes et al. (1985)].

The slowing down and the late evolution of the weak double layer cannot be understood without taking into account the ion dynamics (Chanteur et al., 1983; Chanteur, 1984). Figures 4a and b are local representations of the ion phase space just around the double layer for the above-mentioned particle and Vlasov simulations, respectively. It again emphasizes the similarity of the two runs. In the beginning, the negative pulse of potential is moving subsonically ($\sim 0.8\ c_s$) toward the right in Figures 1 and 2, consistently with the negative velocity perturbation seen at times 320 and 340 in Figures 4a and b.. The pulse first undergoes a very faint slowing down (Chanteur et al., 1983) of purely hydrodynamic origin because of the extremely small number of resonant ions. It has been emphasized in Chanteur (1986) that resonant ions are by no means responsible for this slowing down and the point can be stated in the following way. Weakly nonlinear ion-acoustic waves in a stable plasma with a large electron-to-ion temperature ratio are well accounted for by assuming a cold fluid behavior of the ions and a Boltzmannian distribution of the electrons in the electrostatic potential. The evolution of the potential is then determined by a Korteweg-de Vries (KdV) equation, and the numerical integration of this evolution equation shows that a localized and rarefactive ion-acoustic wave is very slightly slowed down, and simultaneously weakly damped by the radiation of a dispersive tail on its trailing edge (Nishihara et al., 1982; Fornberg and Whitham, 1978; Okutsu and Nakamura, 1979). In the unstable case presently under investigation, the alteration of the pulse by the reflection of the electrons has been incorporated in a dissipative KdV equation (Nishihara et al., 1982; Chanteur et al., 1983). The resulting amplification strengthens the deceleration of the pulse caused by the quadratic nonlinearity $\phi\ (\partial\phi/\partial x)$ of the evolution equation (Nishihara et al., 1982). Of course, the validity of this dissipative KdV equation relying on a fluid description of the ions progressively breaks down with the onset of the ion trapping. The growth of the potential

pulse occurs on a time scale comparable to the transit time of the ion through the pulse; thus, the closer to resonance the ions, the greater the non-adiabatic effect they suffer (which eventually traps them inside the pulse). The onset of the trapping is visible in Figures 4a and b at times 448 and 512, respectively. The transfer of momentum to these ions enhances the slowing down of the pulse, which in turn makes the trapping more efficient as the pulse velocity moves toward the central part of the ion distribution, as shown in Figures 4a and b where the pulse velocity is indicated at each time by a heavy horizontal line. The trapping is completed when the pulse velocity comes to zero, at times around 600 in both simulations; yet, the trapped ions are not phase-mixed inside the pulse, and the highly asymmetric trapped population is responsible for the backward acceleration of the pulse with the subsequent detrapping of the ions. The burst of ions accelerated up to C_s is formed during this process (Fig. 4b) in the downstream region. Such bursts up to 2 C_s are commonly observed in Vlasov simulations started with random initial conditions (Chanteur, 1986). In a two-dimensional system, the trapping acts differently since the ions can enter sideways the potential well, which leads to a trapped population much more symmetric than in one dimension. Barnes et al. (1985) actually observed in two-dimensional simulations that the pulse does not move backward after it has stopped. We can thus conclude that the observed boomerang motion of the structure is an artifact of one-dimensionality.

Except for this rather secondary point, one- and two-dimensional simulations agree on the basic process responsible for the formation of weak double layers driven by the ion-acoustic instability. This process recently received an experimental confirmation in the laboratory experiment done by Sekar and Saxena (1985).

III. AROUND THE MARGINAL STABILITY

It has been suggested in Chanteur (1986) and Pecseli (1984) that the formation mechanism discussed at length in Section II can work with electron drift velocities unable to destabilize the ion-acoustic mode. A series of Vlasov simulations have been done to check that point. More generally, we have studied both subthermal and superthermal drift cases, but always near or below the marginal stability of the plasma. The marginal stability condition referred to is the classical one computed for an infinitesimal harmonic perturbation of the plasma and thus, strictly speaking, is not of concern for the initial condition used to start the simulations. Nevertheless, it indicates that the thermal noise, absent in the Vlasov simulation, would be marginally stable. We chose the same initial condition previously used in Chanteur et al. (1983) and Chanteur (1984) and reported to in the preceding section, i.e., a 10 percent density dip on both species. The drift motion of the electrons relative to the ions rapidly creates a potential trough, the depth of which strongly depends on the drift velocity V_d and on the initial amplitude of the density dip. It is worth noticing that the weak double layers triggered by initial density dips almost vanish when the initial amplitude of these dips is reduced to 1 percent. Thus, under marginally stable conditions, the formation mechanism of weak double layers needs a rather strong initial depression of the plasma density to be effective. In this respect, the linear instability helps a lot in the unstable case. In the present case, the initial density dip has to be produced by other means. The length of the system has been chosen equal to 1024 λ_D and 2048 λ_D in some cases to prevent an early influence of the periodic boundary conditions in the circulating electrons. As said in the introduction, we only present a small sample of our simulation results. A full account of these results will be given in the paper by Verga et al. (1986), presently under preparation. The physical parameters of the five selected runs are listed in Table 1. Figures 5 to 8 illustrate runs 1 to 4, respectively, each figure being composed of an upper panel for the electric potential (averaged over two plasma periods) in unit T_e/e, and of a lower panel for the electron phase space. The results are conveniently organized with respect to the ion-to-electron temperature ratio.

TABLE 1. PHYSICAL PARAMETERS OF THE SELECTED RUNS

Run Number	T_i/T_e	V_c/V_{th}	V_d/V_{th}	Linearly Stable?	System Length (λ_D)
1	0.30	0.55	0.50	yes	1024
2	0.30	0.55	0.60	no	1024
3	0.50	0.88	0.85	yes	1024
4	1.00	1.44	1.25	yes	1024
5	1.00	1.44	1.50	no	2048

Note: The mass ratio is $m_i/me_e = 100$ for the five runs, and V_c is the critical electron drift which destabilizes the plasma.

The case of relatively cold ions ($T_i/T_e = 0.30$) is illustrated by runs 1 and 2, which are linearly stable and unstable, respectively, but both marginally, as appears from Table 1. The two upper panels in Figures 5 and 6 show that the electric potential in the vicinity of the moving density depression has the same spatial variation as the one discussed in Section II for strongly unstable cases. Only quantitative differences occur; the amplitude of the negative pulse and the difference of potential between the downstream (on the right of the figures) and upstream sides which were of the order of one in the Section II cases are now reduced to 0.05 for run 1 and 0.10 for run 2. It is worth noticing that the linear instability, although weak, helps building a difference of potential which is twice the one of the stable case. The electron phase spaces drawn with the same contour levels (lower panels in Figs. 5 and 6) show the same enhancement of the structure; moreover, tiny electron holes are formed downstream of the double layer in run 2. These electron holes can be associated one to one with the small positive pulses seen on the high potential side (Fig. 6, upper part). Run 3 for $T_i/T_e = 0.50$ differs from run 1 by the formation of electron holes, which are even deeper than in run 2, as shown by the phase space (Fig. 7, lower part) and the associated pulses of potential, also more pronounced than in case 2. The potential trough and jump have values twice those of the corresponding values in run 1. Going on to higher ion temperature with $T_i/T_e = 1$, a superthermal drift velocity is now required to get the marginal stability of the plasma, and differences with the colder ion cases can be seen both on the potential and in the electron phase space. First, the potential trough is not as sharp as in the previous cases. Second, the difference of potential, although greater than previously, is much less steep, apart from the large pulses associated with very deep electron holes. Correspondingly, the acceleration region of the electrons in the vicinity of the potential well (see Fig. 8, lower part) is not as well defined as in the cold ion case. To briefly summarize the observations, we can say that, except for very weak drift velocities, electron holes moving at velocities close to $0.5\ V_{th}$ are recurrently formed in the density depression which moves subsonically. The region of high potential extends between the density depression and the leading electron hole.

Run 5 differs from run 4 by the initial condition, which is now made of two identical density depressions separated by $512\ \lambda_D$. Snapshots of the averaged potential presented in Figure 9 show that the two structures evolve independently, as long as they are disconnected, yet a blowup of the potential occurs when the two depleted regions join together. This behavior has not yet been investigated in detail and needs to be confirmed for other sets of parameters.

IV. CONCLUSION

The physics of the formation of weak double layers by current interruption seems now to be satisfactorily understood after a few years of both theoretical and numerical work. We have presented the first evidence of weak double layer formation in stable conditions: they share conditions, except for those associated to the ion dynamics. Their weakness explains why they have almost no effect in the ion phase space. An interesting point associated with these structures is the recurrent formation of electron holes; we believe that it deserves further work, as well as the blowup of the field observed during the coalescence of two depleted regions.

Acknowledgments. The author greatly acknowledges the organizing committee of the Workshop on Double Layers in Astrophysics for financial support. The scientific collaboration of R. Pellat and A. Verga has been greatly appreciated. The author is also grateful to N. Dupin for her careful reading and efficient typing of the manuscript.

REFERENCES

Barnes, C., M. K. Hudson, and W. Lotko, *Phys. Fluids, 28,* 1055 (1985).
Berman, R. H., D. J. Tretault, and T. H. Dupree, *Phys. Fluids, 28,* 155 (1985).
Borovsky, J. E., in *Second Symposium on Plasma Double Layers,* edited by R. Schrittwieser and G. Eder, University of Innsbruck, p. 33, 1984.
Chanteur, G., in *Computer Simulation of Space Plasmas,* edited by H. Matsumoto and T. Sato, Terra Scientific Publ Co., p. 279, 1984.
Chanteur, G., in *Proceedings of the International Conference on Comparative Study of Magnetospheric Systems,* Cepadues Editions, Toulouse, to appear, 1986.
Chanteur, G., J. C. Adam, R. Pellat, and A. S. Volokhitin, *Phys. Fluids, 26,* 1584 (1983).
DeGroot, J. S., C. Barnes, A. E. Walstead, and O. Buneman, *Phys. Rev. Lett., 38,* 1283 (1977).
Dupree, T. H., *Phys. Fluids, 26,* 2460 (1983).
Fornberg, B., and G. B. Whitham, *Phil Trans. Roy Soc. London, A, 289,* 373 (1978).
Hasegawa, A., and T. Sato, *Phys. Fluids, 25,* 632 (1982).
Hudson, M. K., and D. Potter, in *Physics of Auroral Arc Formation,* Geophys. Monogr. Series #25 (American Geophysical Union: Washington, D.C.), p. 260 (1981).
Hultqvist, B., *Planet. Space Sci., 19,* 749 (1971).
Ishiguro, S., T. Kamimura, and T. Sato, *Phys. Fluids, 28,* 2100 (1985).
Kindel, J. M., C. Barnes, and D. W. Forslund, in *Physics of Auroral Arc Formation,* Geophys. Monogr. Series #25 (American Geophysical Union: Washington, D.C.), p. 296, 1981.
Nishihara, K., H. Sakagami, T. Taniuti, and A. Hasegawa, in *First Symposium on Plasma Double Layers,* edited by P. Michelsen and J. J. Rasmussen, p. 41, Risoe National Laboratory, Denmark, 1982.
Okuda, H., and M. Ashour-Abdalla, *Phys. Fluids, 25,* 1564 (1982).
Okutsu, E., and Y. Nakamura, *Plasma Physics, 21,* 1053 (1979).
Pécseli, H., in *Second Symposium on Plasma Double Layers,* edited by R. Schrittwieser and G. Eder, University of Innsbruck, p. 81, 1984.
Sato, T., and H. Okuda, *Phys. Rev. Lett., 44,* 740 (1980).
Sato, T., and H. Okuda, *J. Geophys. Res., 86,* 3357 (1981).
Sekar, A. N., and Y. C. Saxena, *Plasma Physics and Controlled Fusion, 27,* 181 (1985).
Serizawa Y., and T. Sato, *Geophys. Res. Lett., 11,* 595 (1984).
Singh, N., and R. W. Schunk, in *Second Symposium on Plasma Double Layers,* edited by R. Schrittwieser and G. Eder, University of Innsbruck, p. 364, 1984.
Singh, N., H. Thiemann, and R. W. Schunk, *J. Geophys. Res., 90,* 5173 (1985).
Verga, A., G. Chanteur, and R. Pellat, in preparation (1986).

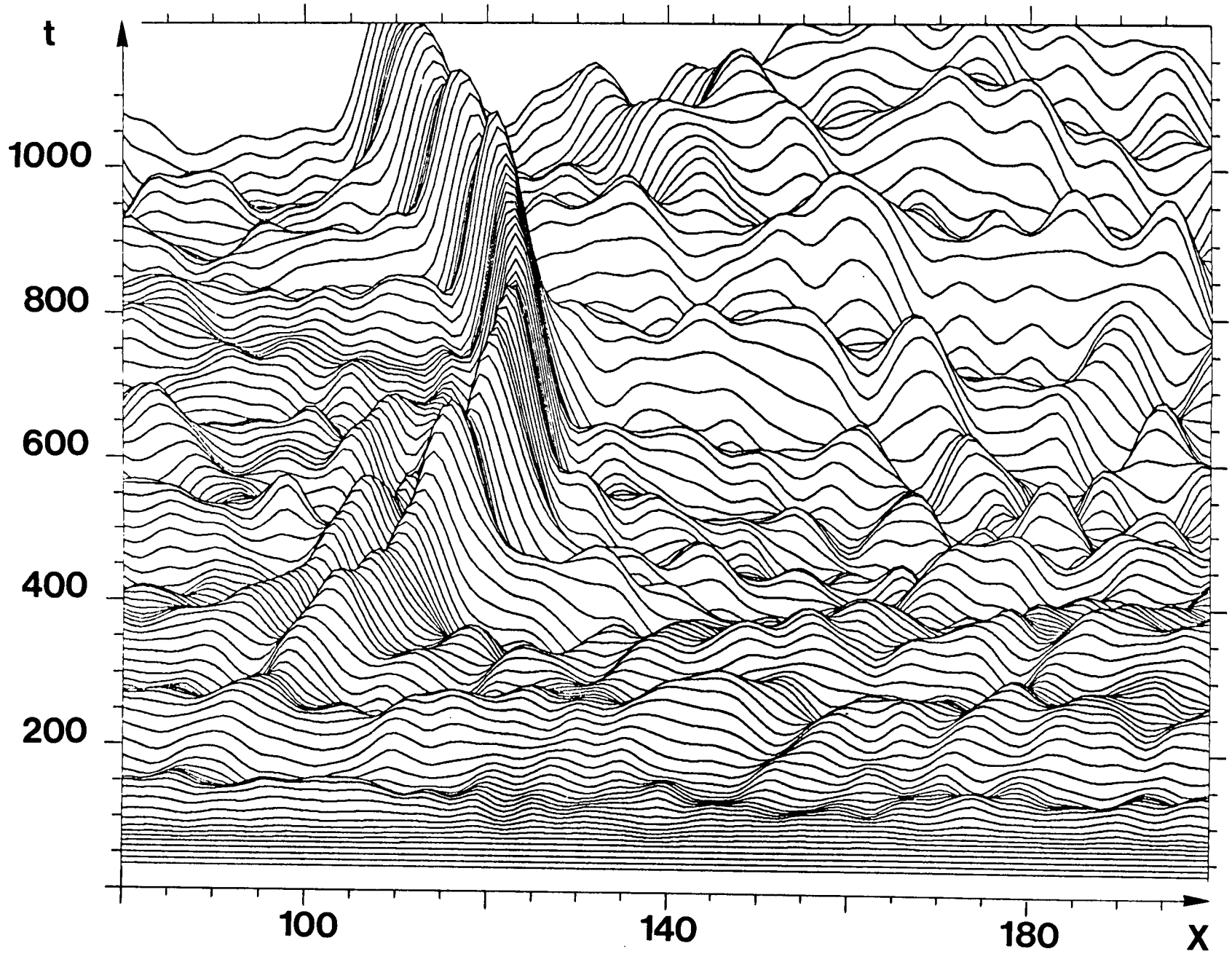

Figure 1. Potential energy of an electron versus x and t in the vicinity of the moving density dip (particle simulation).

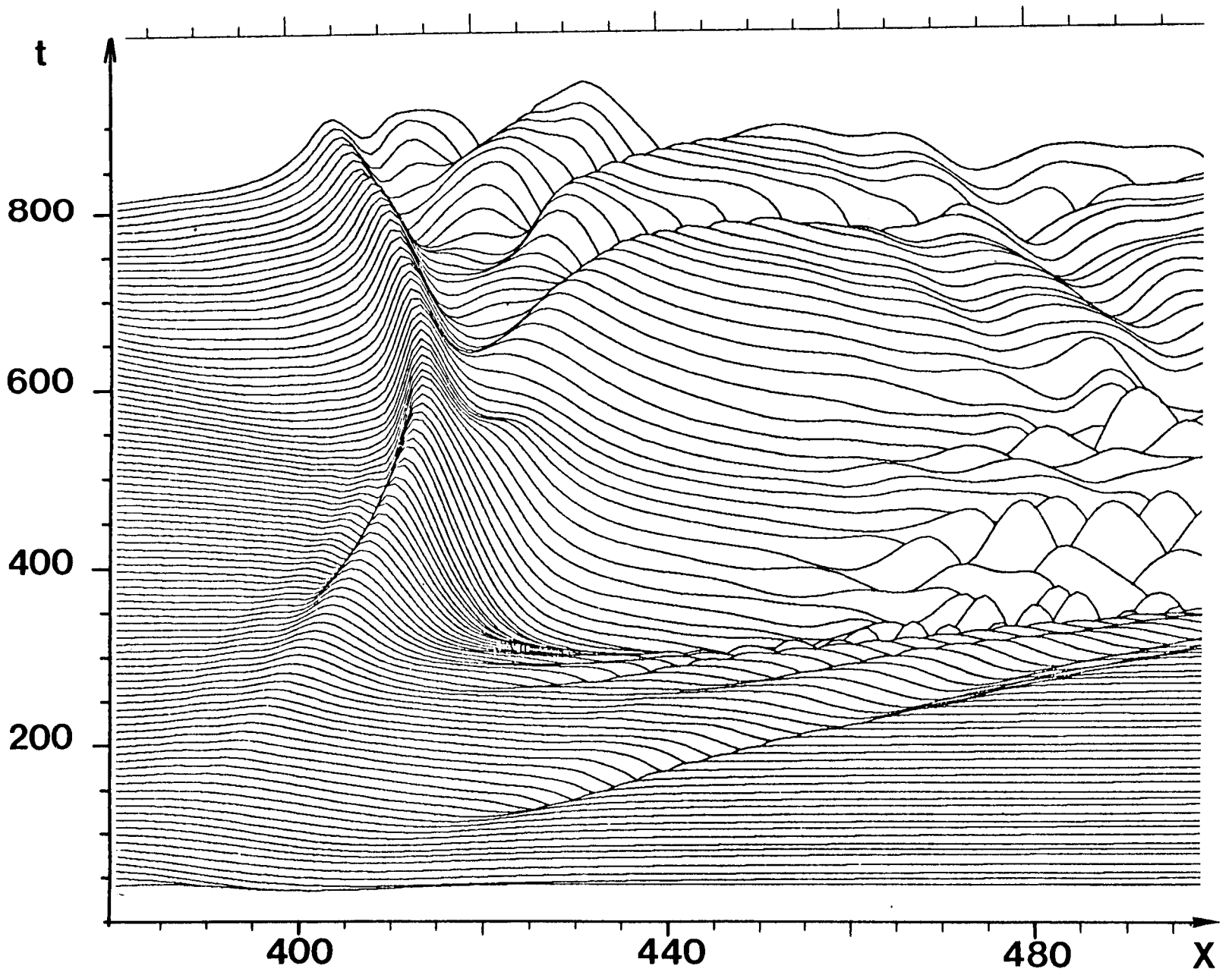

Figure 2. Same as Figure 1 but for the Vlasov simulation.

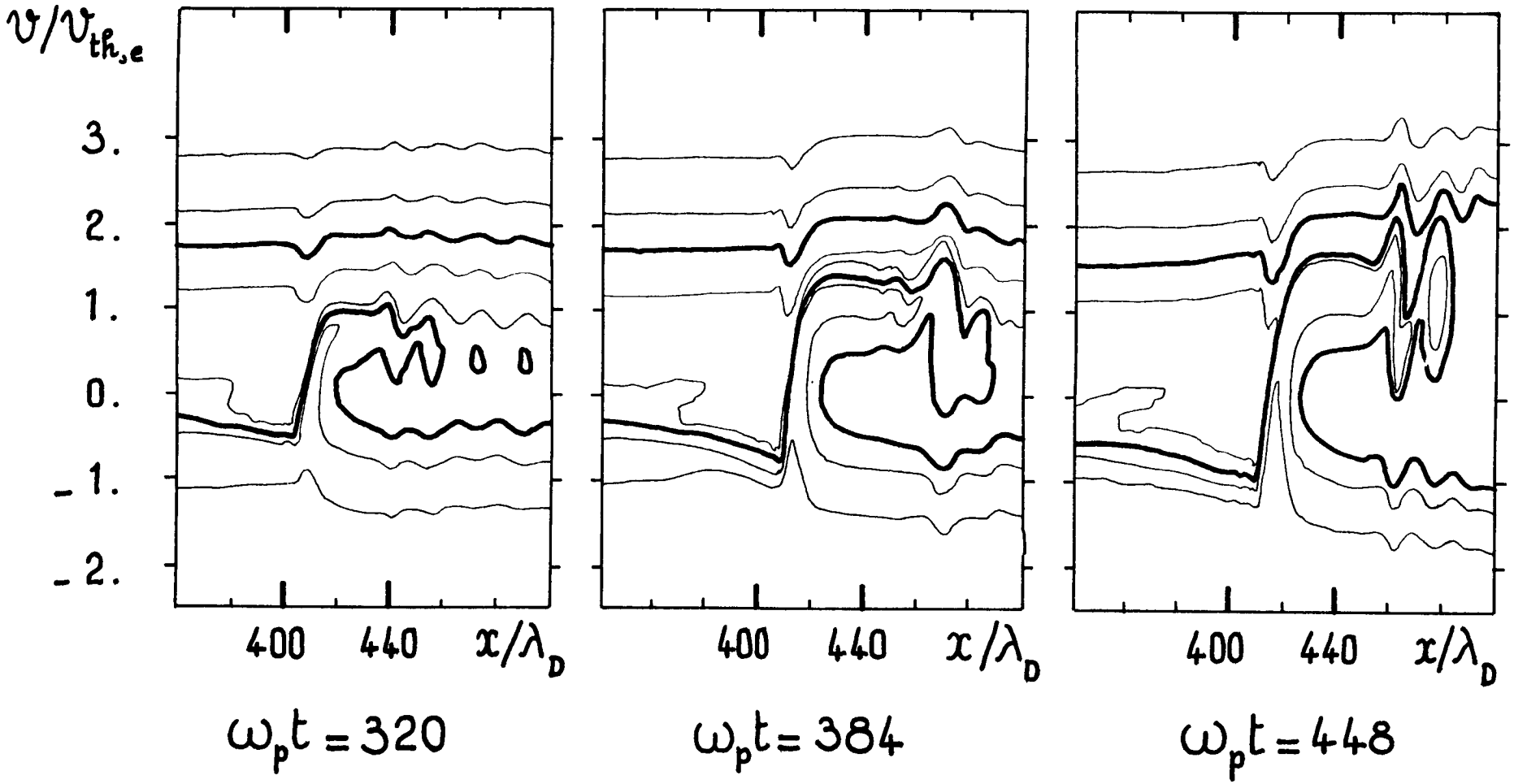

Figure 3. Electron phase space at three different times in the vicinity of the double layer at three different times (Vlasvos simulation).

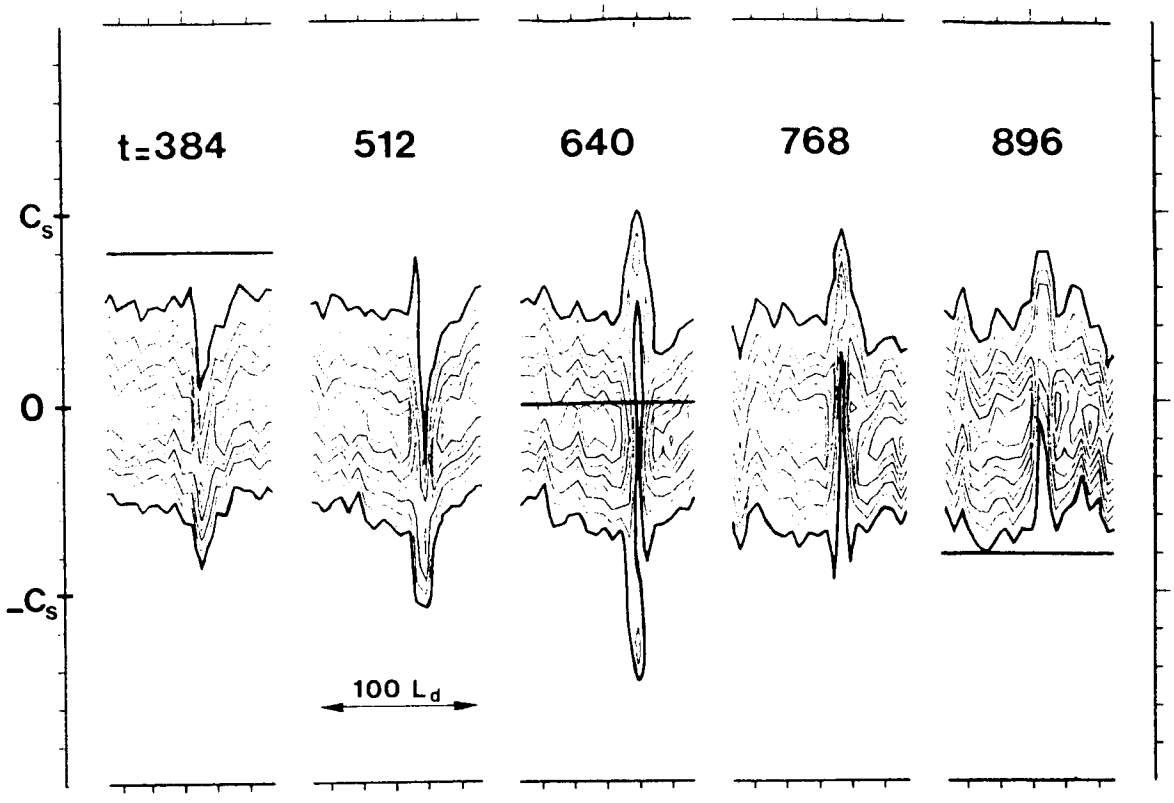

(a)

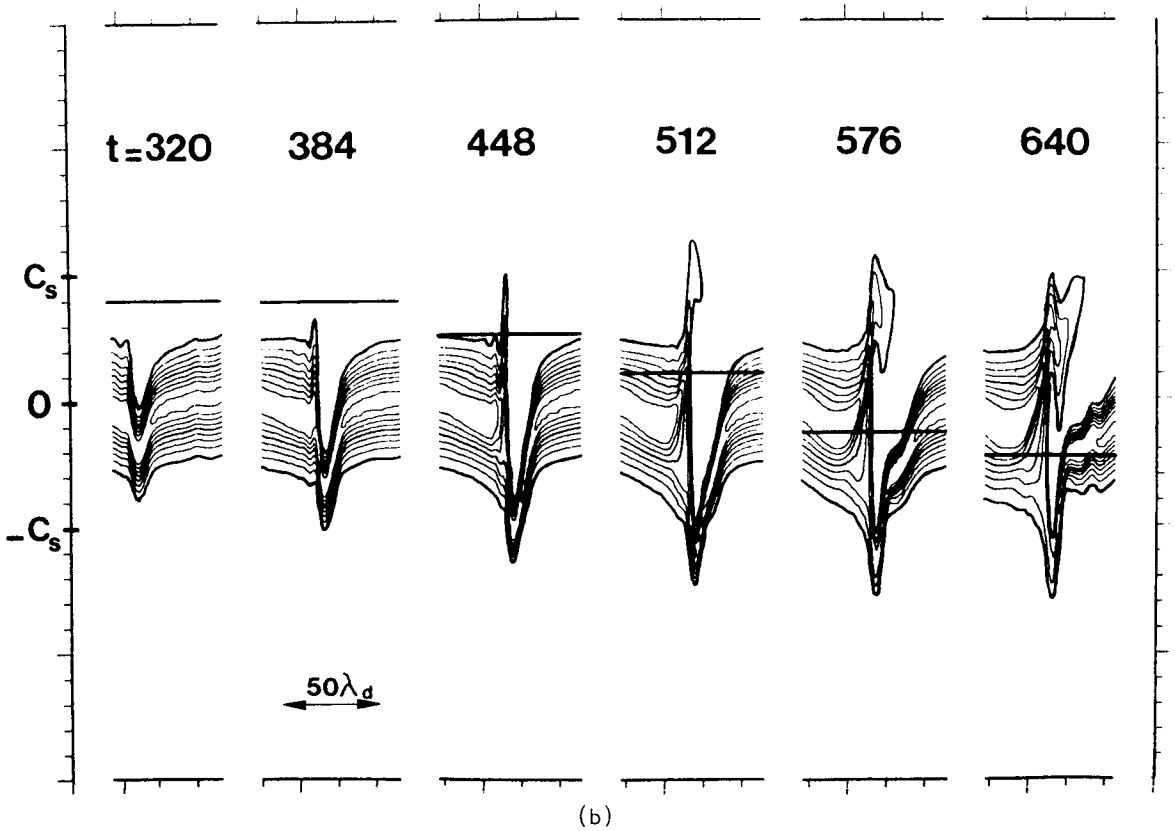

(b)

Figure 4. Ion phase spaces around the double layer at different times. (a) Particle simulation; (b) Vlasov simulation. The heavy horizontal line indictes the velocity of the localized wave.

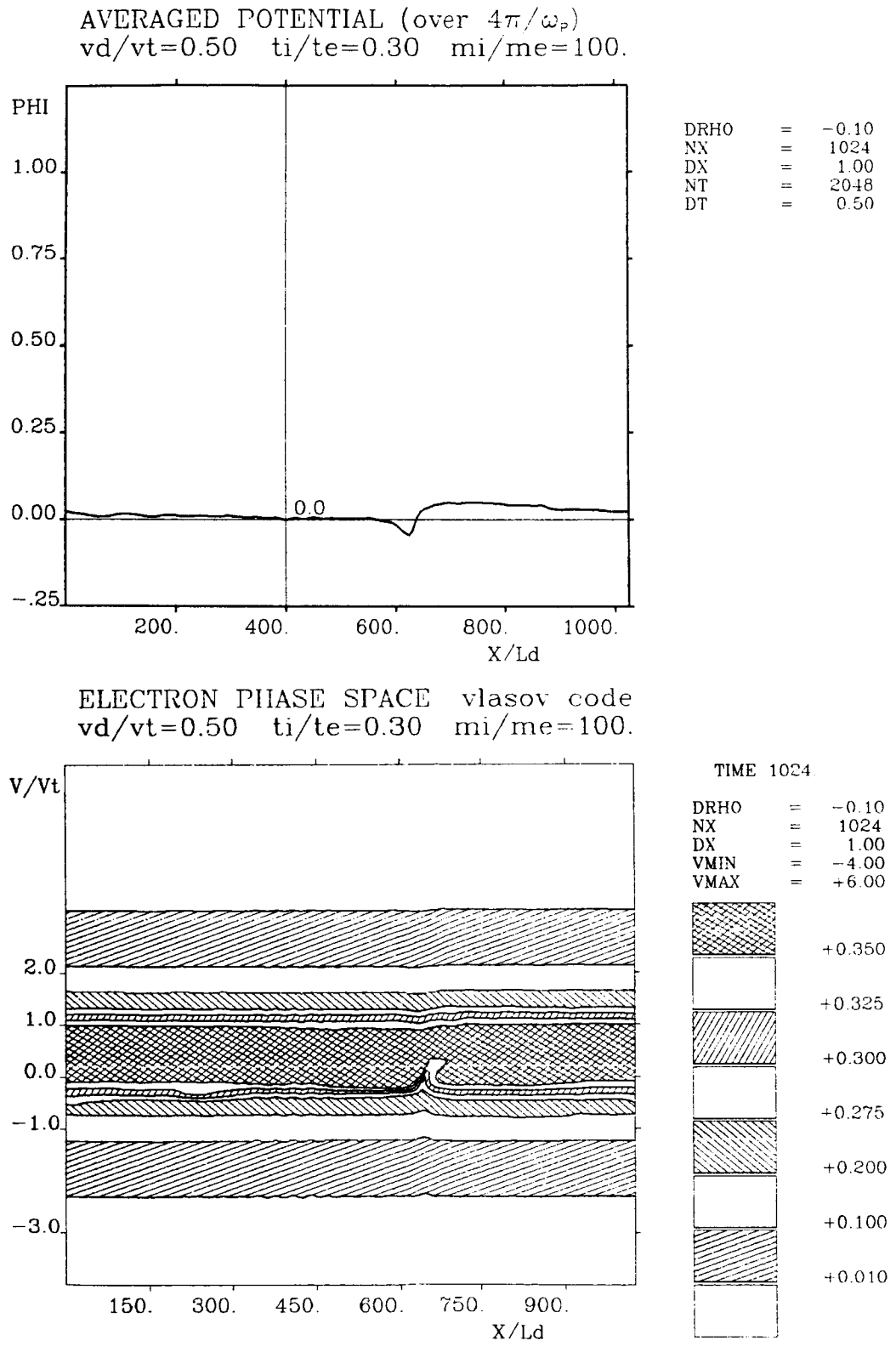

Figure 5. Upper: averaged electrostatic potential around t = 1024 for run 1 of Table 1. Lower: corresponding electron phase space.

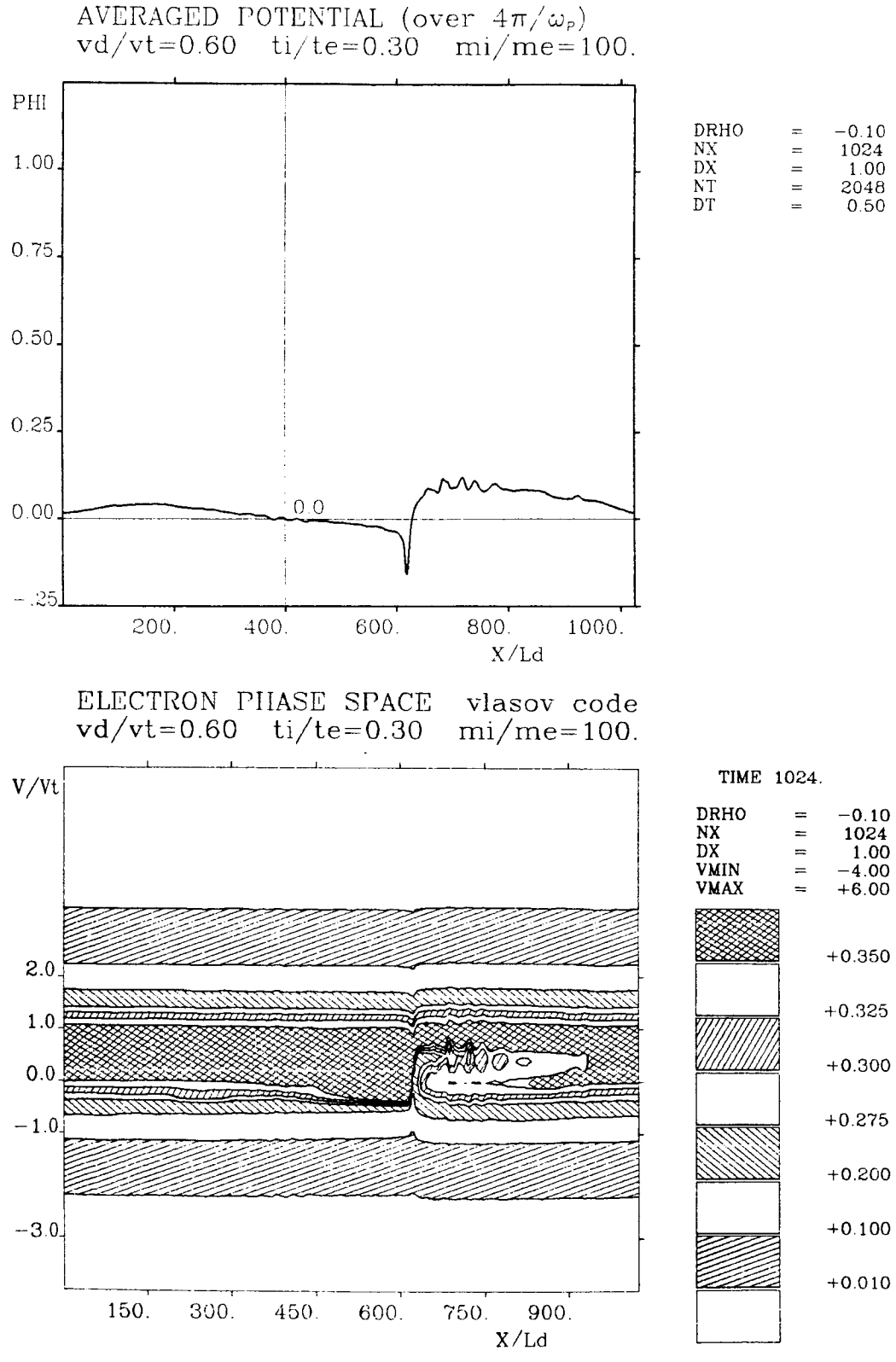

Figure 6. Same as Figure 5 for run 2.

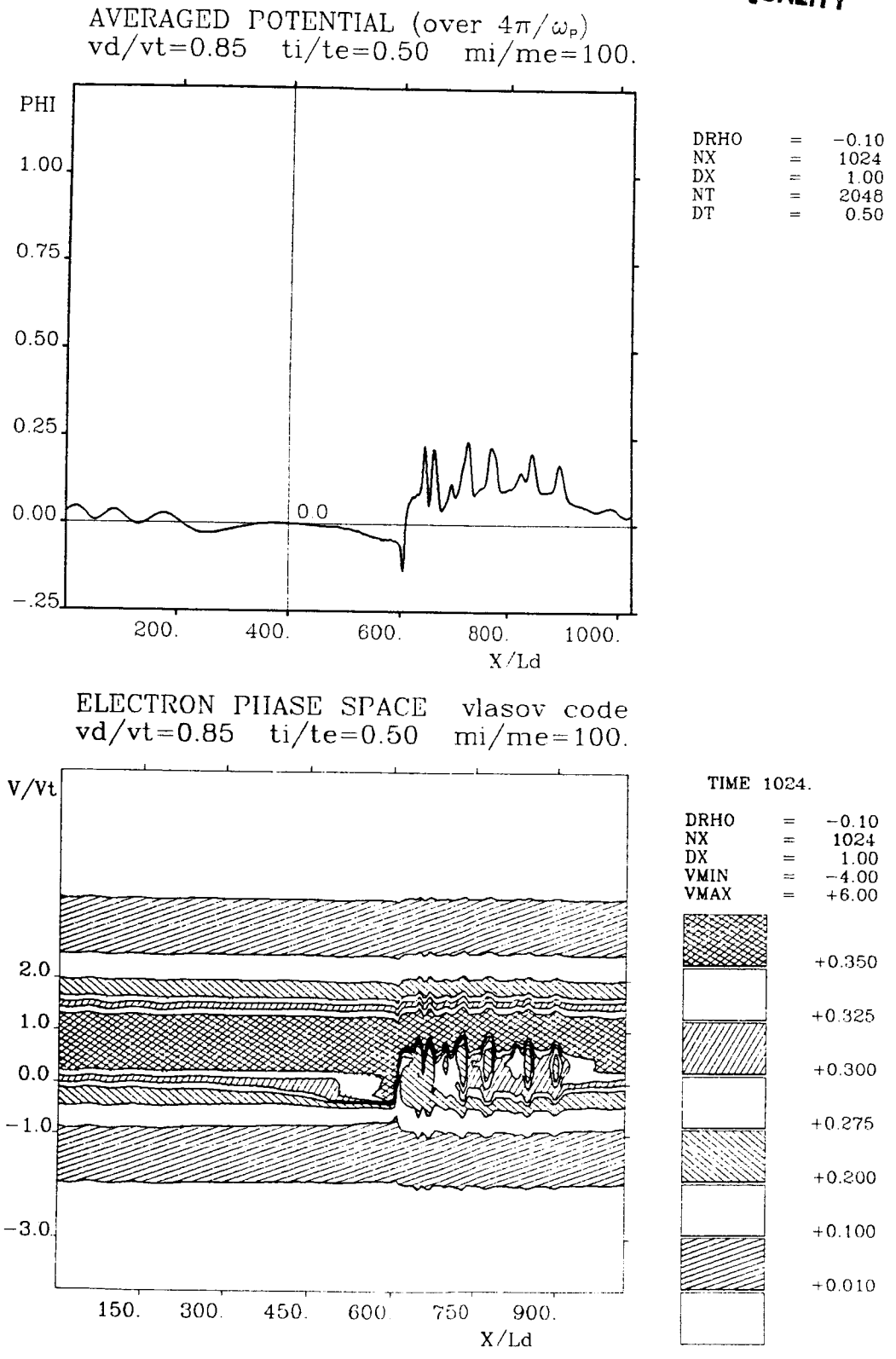

Figure 7. Same as Figure 5 for run 3.

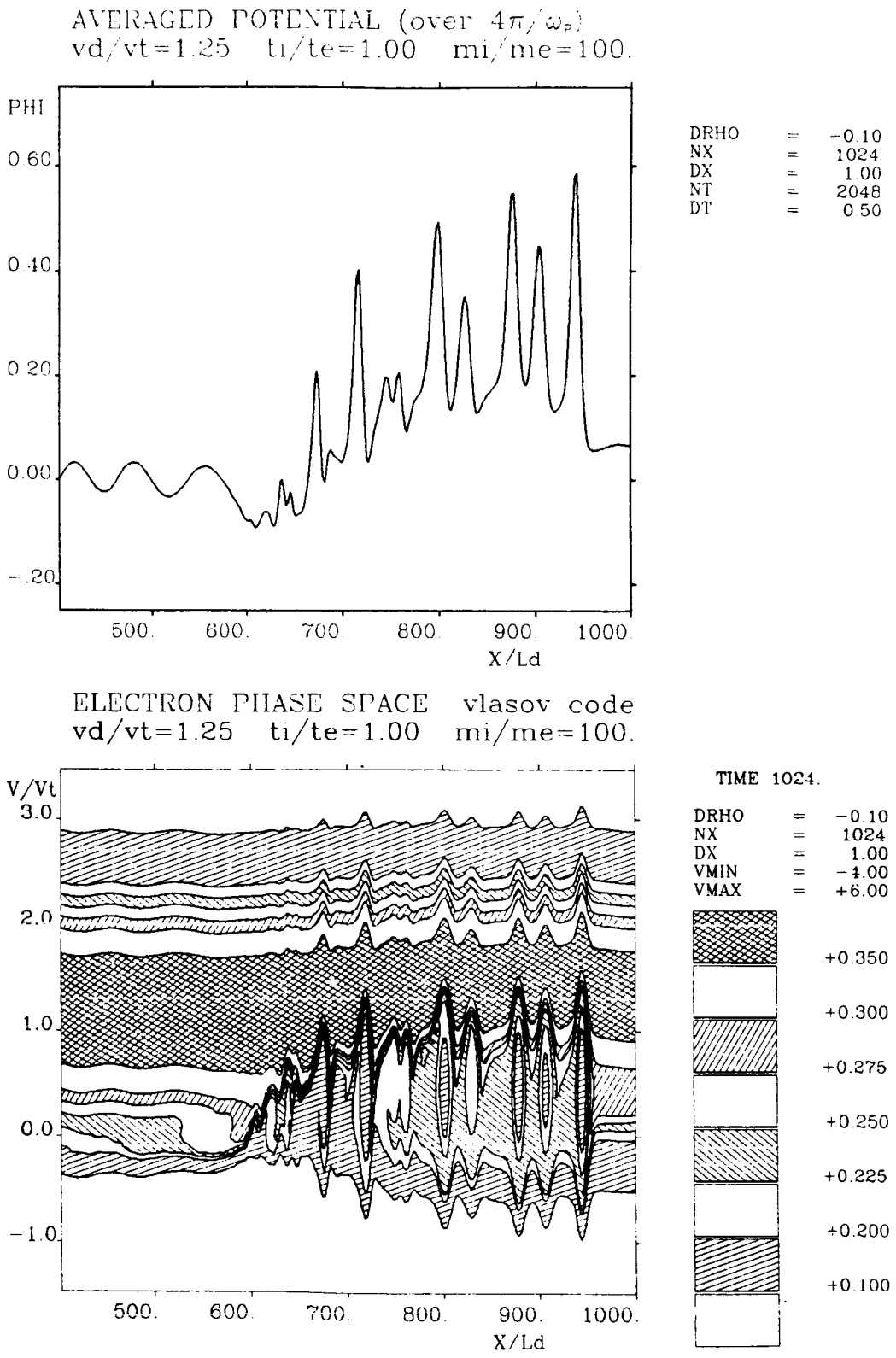

Figure 8. Same as Figure 5 for run 4.

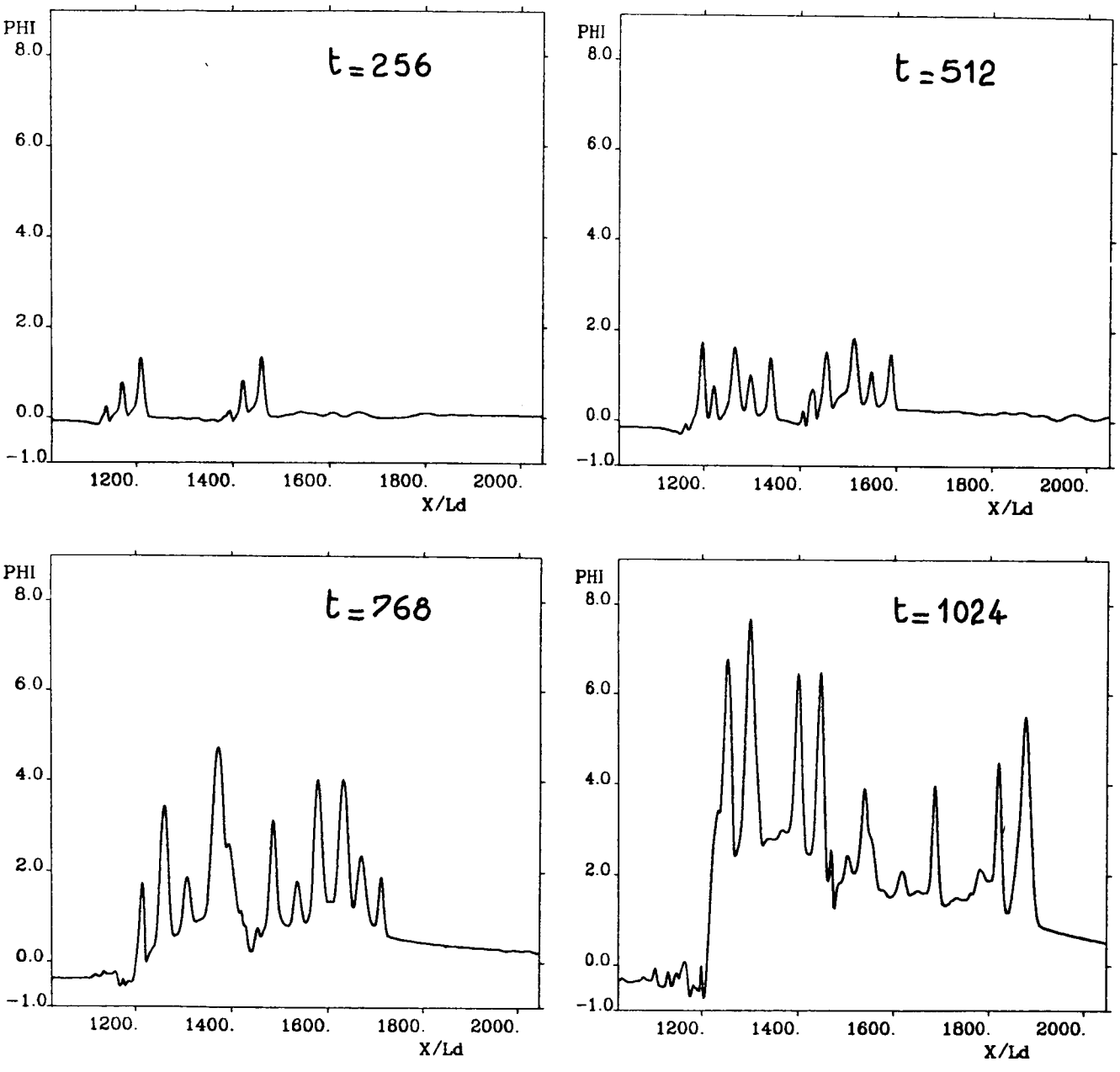

Figure 9. Averaged electric potential at times 256, 512, 768, and 1024 ω_{pe}^{-1} for run 5. Notice the blowup of the potential after time 768.